

Effects of Surface Roughness on Lossy Rectangular Waveguide

Juan Chen and Binke Huang

School of Electronic and Information Engineering, Xi'an Jiaotong
University, Xi'an 710049, China
chenjuan0306@yahoo.com.cn

Abstract — The integral equation method combined with the surface-impedance boundary condition is applied for the analysis of propagation characteristics of rough lossy metal waveguides. The surface roughness of waveguide is random, and the statistical properties associated to the wall roughness are consistent with a Gaussian random process. The effects of the waveguide parameters on the propagation constant and attenuation constant are discussed rigorously, including the frequency, the standard deviation of height and correlation length of the Gaussian roughness. The results show that, as the increases of correlation length and frequency, the propagation constant is increased and the attenuation constant is decreased; while as the increase of the standard deviation, the trends of the propagation constant and the attenuation constant are just opposite.

Index Terms — Gaussian random process, integral equation, rectangular waveguide, rough surface, surface-impedance boundary.

I. INTRODUCTION

The surface roughness of waveguide is a practical reality. It may occur due to various reasons, such as polishing of irregular waveguide structures, uneven surface coating or corrugation of surface while fabricating the waveguides. The problem of roughness may also arise due to exposure of waveguide to environment. The environmental corrosion increases with ageing which results in increasing roughness of waveguide walls. The surface roughness will affect the propagation constant and attenuation constant of the waveguide, and change the cutoff frequency of every waveguide mode [2], so, it becomes very important to study the effect of

surface roughness on electromagnetic wave propagation.

There have been many numerical techniques presented to study the effect of surface roughness on waveguide [1-9], including full-wave mode-matching method [1], finite element method [2], moments method [3-5], and finite-difference frequency-domain method [6,7]. In [2], the effect of surface roughness on TE₁₀, TE₂₀ mode cutoff frequencies and passbands is studied. In [3], the calculation for TM modes in waveguides with polygonal and fractal cross-sectional shapes is presented; in [4], the case for TE waves of waveguides with inner polygonal structure is considered. Based on the numerical techniques of [3, 4]. In [5], a scheme to generate an ensemble of realizations for wall Gaussian random rough profiles in circular waveguide is proposed, but without considering the attenuation of the lossy metal. The finite-difference frequency-domain method to compute the lossy metal waveguides is used in [6, 7]. In this method, the surface-impedance boundary condition (SIBC) is applied for lossy metal structures. By solving the Eigen equation, the phase constants and attenuation constants can be found for a given frequency. However, this method is confined to solve the regular surface roughness waveguide. In practice, most waveguide is made of imperfect conductor, and is with random surface roughness. Thus, a numerical method which can be applied to simulate the random rough lossy waveguide becomes important.

In this paper, a new integral equation method is presented for the analysis of propagation characteristics of rough lossy metal waveguides. The surface roughness of waveguide is random, and the statistical properties associated to the wall

roughness are consistent with a Gaussian random process. The attenuation of the imperfect conductor is considered by using the surface-impedance boundary condition. The validity of this numerical technique to simulate the case of rough waveguide is confirmed by a comparison with previous results.

The advantage of this integral equation method is that it can be used to analyze the random rough lossy waveguide and compared with the full wave methods, such as the FDTD method and MOM method, this method is easy to program. By using this integral equation method, the effects of the waveguide parameters on the propagation constant and attenuation constant are discussed rigorously, including the conductivity of the lossy metal, the standard deviation of height and correlation length of the Gaussian roughness. Some useful conclusions are reached.

This paper is organized as follows. The numerical technique applicable to calculations of rough lossy waveguides is presented first; then, the validity of the approach is tested by a comparison with previous results. After that, the effects of the parameters of the roughness on the propagation constant and attenuation constant are discussed; and some useful conclusions are reached.

II. NUMERICAL TECHNIQUE

A cylindrical surface S of general cross-sectional contour is shown in Fig. 1. The cross-sectional size and shape are assumed constant along the cylinder axis (z direction), and the intersection of the cylinder with the $x-y$ plane is the closed profile C . We have assumed that the inner space of the cylinder be vacuum.

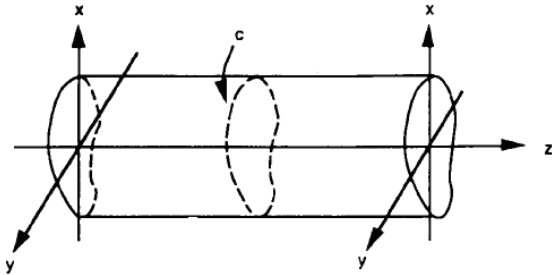


Fig. 1. Hollow cylindrical waveguide of arbitrary cross-sectional shape.

It is a well-known fact that if we assume a sinusoidal time dependence $e^{-i\omega t}$ for the fields

inside the cylindrical waveguide, the basic problem reduces to finding the eigen values γ and the corresponding eigen functions $\psi_\gamma(x, y)$, which represent modes of the electric field E_z (TM-waves) or of the magnetic field H_z (TE-waves). To find these modes, we need to solve the two-dimensional Helmholtz equation,

$$\left(\nabla_T^2 + \gamma^2\right)\psi_\gamma(x, y) = 0. \quad (1)$$

∇_T^2 is given by

$$\nabla_T^2 = \nabla^2 - \partial^2/\partial z^2. \quad (2)$$

The parameter γ can be expressed as,

$$\gamma^2 = \frac{\omega^2}{c^2} + k_z^2, \quad (3)$$

where c is light velocity, k_z is the wavevector component of the electromagnetic wave propagating along the axis of the waveguide.

We introduce a Green's function $G_\gamma(r, r')$, which is the solution of the two-dimensional inhomogeneous Helmholtz equation,

$$\left(\nabla_T^2 + \gamma^2\right)G_\gamma(r, r') = -4\pi\delta(r - r') \quad (4)$$

where $r = (x, y)$ and $r' = (x', y')$. The Green's function can be expressed in terms of a Hankel function as follows:

$$G_\gamma(r, r') = i\pi H_0^{(1)}(\gamma|r - r'|) \quad (5)$$

Applying Green's integral theorem to the functions $\psi_\gamma(r)$ and $G_\gamma(r, r')$, it obtains,

$$\psi_\gamma(r) = \frac{1}{4\pi} \oint_C \left[G_\gamma(r, r') \frac{\partial}{\partial n} \psi_\gamma(r') - \psi_\gamma(r') \nabla' G_\gamma(r, r') \cdot \bar{n} \right] ds \quad (6)$$

where, \bar{n} is the unitary vector normal to each point on C outward.

Considering the finite conductivity of the metal waveguide, we apply the surface-impedance boundary condition along the profile C .

$$E_{tan} = Z_s \bar{n} \times H_{tan} \quad (7)$$

For lossy metal waveguides, $Z_s = (1 + i)/\delta\sigma$, with δ the skin depth, σ the conductivity of metal, and index tan the tangential field components around profile C .

For the TE-waves, $\psi_\gamma = H_z, E_z = 0$. Applying equation (7), we have,

$$\psi_\gamma Z_s = \frac{i\omega\mu}{\gamma^2} \frac{\partial \psi_\gamma}{\partial n}. \quad (8)$$

Introducing equation (8) into equation (6), it obtains,

$$\psi_\gamma(r) = \frac{1}{4\pi} \oint_c \left[G_\gamma(r, r') Z_{TE} \right] \psi_\gamma(r') ds \quad (9)$$

where,

$$Z_{TE} = \frac{Z_s \gamma^2}{i\omega\mu} \quad (10)$$

with the same manipulation, the integral equation for the TM-waves is,

$$\psi_\gamma(r) = \frac{1}{4\pi} \oint_c \left[G_\gamma(r, r') Z_{TM} \right] \psi_\gamma(r') ds \quad (11)$$

with,

$$Z_{TM} = \frac{i\gamma^2}{Z_s \omega \epsilon} \quad (12)$$

To determine the Eigen values γ and the correspondence source functions $\psi_\gamma(r)$, we convert the integral equations (9) and (11) into a matrix equation by using a simple rectangular approximation to evaluate the integrals over small intervals. This matrix equation can then be solved numerically.

The matrix equation for the source function $\psi_\gamma(r)$, is given by,

$$0 = \sum_{n=1}^N L_{mn}^\gamma \psi_\gamma^n \quad m = 1, 2, \dots, N \quad (13)$$

where, $\psi_\gamma^n = \psi_\gamma(r)|_{r=r(c_n)}$ and $r(c_1), r(c_2), \dots, r(c_N)$ are N equally spaced points on the contour. The explicit expression for the matrix elements can be obtained [5],

$$L_{mn}^\gamma = \left[\begin{array}{c} \frac{i\Delta s}{4} H_0^{(1)}(\gamma d_{mn})(1 - \delta_{mn}) \\ -\frac{\Delta s}{4i} H_0^{(1)}\left(\gamma \frac{\Delta s}{2e}\right) \delta_{mn} \end{array} \right] Z$$

$$-\frac{i\Delta s}{4} \left\{ \gamma \frac{H_1^{(1)}(\gamma d_{mn})}{d_{mn}} \times \begin{pmatrix} X_n' [Y_m - Y_n] \\ -Y_n' [X_m - X_n] \end{pmatrix} \right\} (1 - \delta_{mn}) \\ + \left\{ \frac{1}{2} - \frac{\Delta s}{4\pi} (X_n' Y_n'' - X_n'' Y_n') \right\} \delta_{mn} \quad (14)$$

with

$$d_{mn} = \left\{ [X_m - X_n]^2 + [Y_m - Y_n]^2 \right\}^{1/2},$$

where Δs is the distance on curve C between $r(c_j)$ and $r(c_{j+1})$,

with $j = 1, 2, \dots, N - 1$; (X_m, Y_m) are the Cartesian components of the vector $r(c_m)$, and

$H_1^{(1)}(z)$ is a Hankel functions of first order; each prime symbol denotes a derivative. For the TE and TM-waves, $Z = Z_{TE}$ and Z_{TM} , respectively.

As can be observed from equation (13), the matrix equation is homogeneous; thus, the values of γ can be determined from the condition,

$$|L_{mn}^\gamma| = 0 \quad (15)$$

We define the function

$$D(\gamma) = \ln(|L_{mn}^\gamma|) \quad (16)$$

considering that the logarithm function is appropriately convenient. Because of numerical limitations, condition (15) is satisfied approximately for eigenvalues $\gamma_1, \gamma_2, \dots$, where $D(\gamma_1), D(\gamma_2), \dots$ are minima of the $D(\gamma)$ function.

The source function ψ_γ^n can be determined by using a singular-value-decomposition numerical technique [8], with use of equation (13), which represents a set of homogeneous equations, where the matrix L_{mn}^γ is numerically close to singular.

Once γ and the source function ψ_γ^n have been determined, the field amplitude in the cylinder can be calculated,

$$\psi_\gamma(x, y) = \frac{i\Delta s}{4} \sum_{n=1}^N \psi_\gamma^n \left(\begin{matrix} H_0^{(1)}(\gamma d_n) Z \\ -\gamma \frac{H_1^{(1)}(\gamma d_n)}{d_n} \times \begin{pmatrix} x_n [y - y_n] \\ -y_n [x - x_n] \end{pmatrix} \end{matrix} \right) \quad (17)$$

with $d_n = \left\{ [x - x_n]^2 + [y - y_n]^2 \right\}^{1/2}$.

III. VALIDATION

In this section, the numerical technique presented above is validated by a comparison with previous results.

A metal rectangular waveguide with width $a = 19.05$ mm, height $b = 9$ mm, and conductivity $\sigma = 5.8 \times 10^7$ S/m (the conductivity of copper) is considered [7]. Wavevector component $k_z = \alpha + j\beta$, with β the propagation constant, and α the attenuation constant. The numerical results of β and α with respect to frequency calculated by the integral equation method are presented in Fig. 2 and 3. For comparison, the results of [7] are also shown in these figures. It can be seen from these figures that, the numerical results calculated by using the integral equation method agree well with the results of [7].

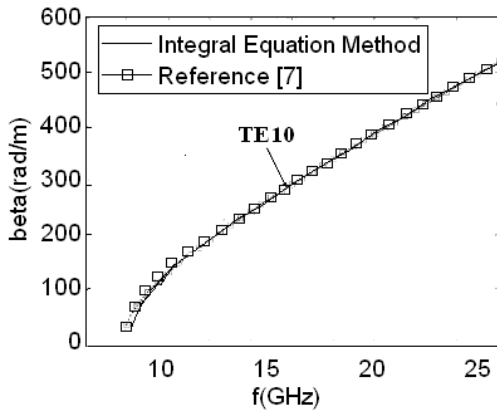


Fig. 2. Propagation constant β of a metal empty rectangular waveguide.

IV. DISCUSSION

By using the numerical technique presented above, we discuss the effects of the waveguide parameters on the propagation constant and

attenuation constant, including the conductivity σ of the lossy metal, the standard deviation of height D and correlation length l_{co} of the Gaussian roughness. The ensembles of profiles with these statistical properties are generated by using the method presented in [5]. Considering the randomness, we take into account one hundred realizations for a calculation; then, we get the statistical average value of these results.

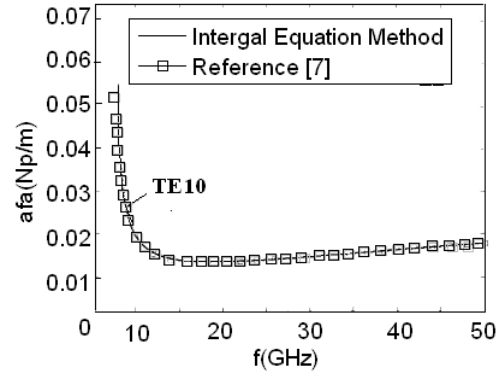


Fig. 3. Attenuation constant α of a metal empty rectangular waveguide.

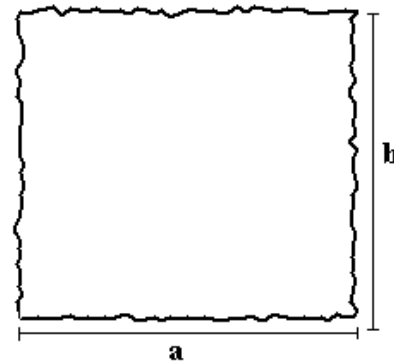


Fig. 4. Simplified model for rectangular waveguides with Gaussian rough surface

The dimension of the rough waveguide is $a = b = 8$ mm, as shown in Fig. 4. In this figure, both the standard deviation of height D and correlation length l_{co} are equal to 0.01mm.

A. Effect of the conductivity σ

Supposing the waveguide is regular ($D = 0$), and keeping the work frequency unchanged, by using the integral equation method, we can get the variations of the propagation constant β and attenuation constant α with respect to waveguide

conductivity σ , as shown in Figs. 5 and 6. Here, we consider the first four modes of the regular waveguide: TE₁₀, TE₁₁, TM₁₁, and TM₂₁ modes.

It can be seen from Fig. 5, that as the increase of the conductivity σ , the propagation constants β of the TE modes are increased, and the propagation constants β of the TM modes are decreased. The attenuation constants α , both for the TE modes and TM modes, are all decreased as the increase of conductivity σ , as shown in Fig. 6. Besides, it can be seen from these two figures that when the conductivity σ increase to 75dbS/m (about 5.8×10^7 s/m, the conductivity of copper), the variations of the propagation constant β and attenuation constant α with respect to conductivity σ are not obvious, which means that, when exceeding the conductivity of copper, the effect of σ on the propagation performance of the waveguide is not considerable.

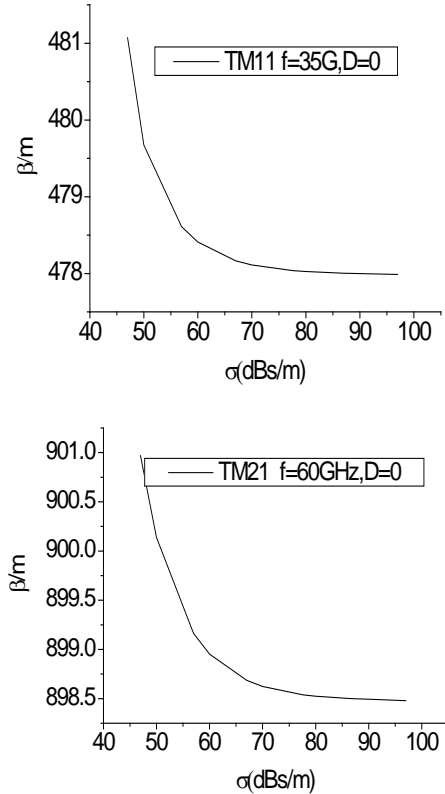
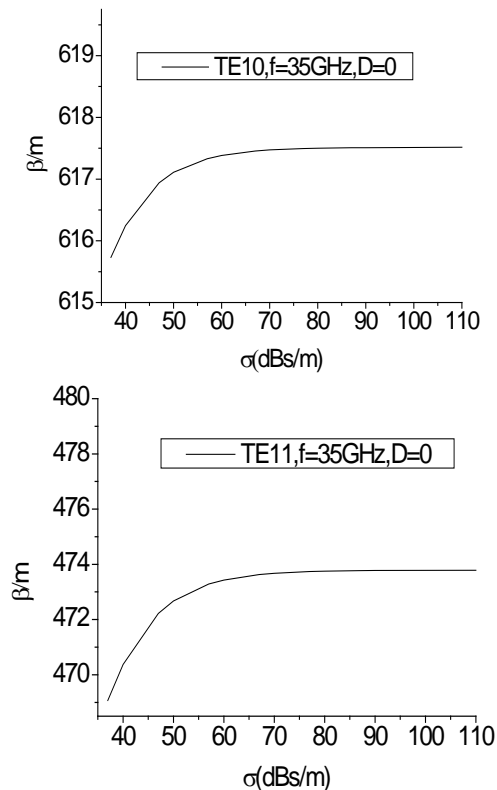


Fig. 5. The variations of the propagation constant β with respect to conductivity σ .

B. Effect of the standard deviation of height D

We let the conductivity of the waveguide $\sigma = 5.8 \times 10^7$ S/m, the correlation length $l_{co} = 0.05$, and keep the work frequency unchanged. In this section, we discuss the effects of the standard deviation of height D of the Gaussian rough waveguide on the propagation constant β and attenuation constant α .

By using the integral equation method, we can get the variations of propagation constant β and attenuation constant α with respect to standard deviation of height D , as shown in Figs. 7 and 8. It can be seen from these two figures that, as the increase of D , for both the TE and TM modes, the propagation constants β are decreased and the attenuation constants α are increased.

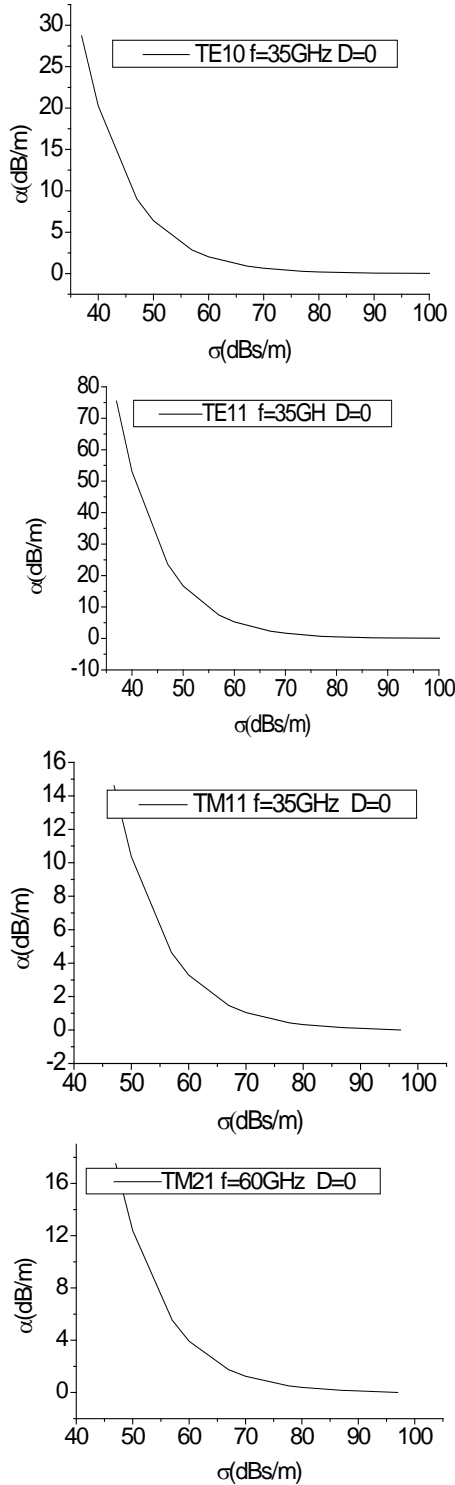
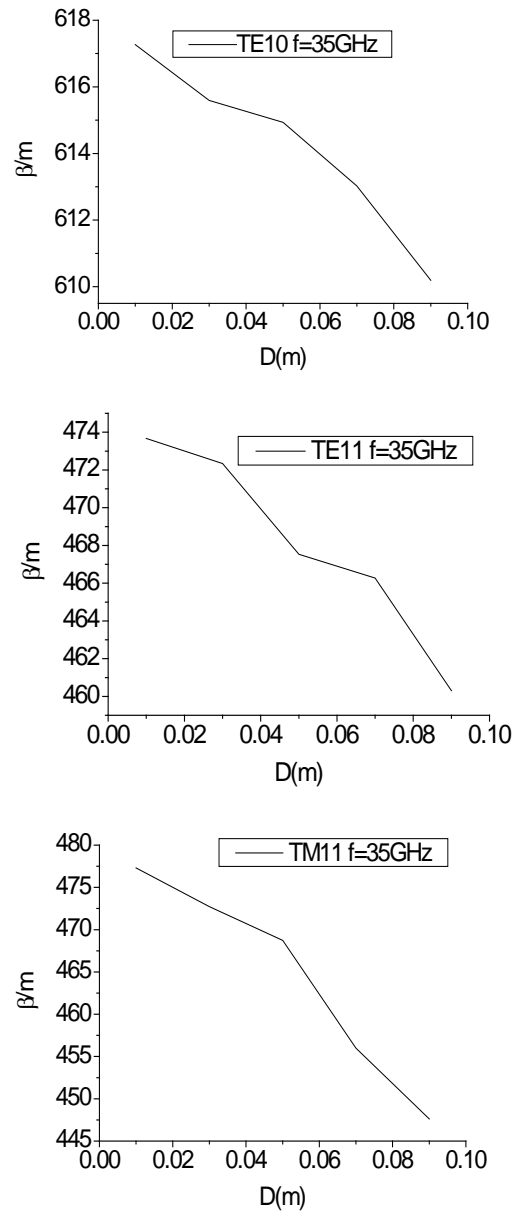


Fig. 6. The variations of attenuation constant α with respect to conductivity σ .

C. Effect of the correlation length l_{co}

Supposing the conductivity of the waveguide $\sigma = 5.8 \times 10^7$ S/m, standard deviation of

height $D=0.03$, and keeping the work frequency unchanged, by using the integral equation method, we can get the propagation constant β and attenuation constant α for different correlation length l_{co} , as shown in Figs. 9 and 10. It can be seen from these figures that, as the increase of l_{co} , for both the TE and TM modes, the propagation constants β are increased and the attenuation constants α are decreased.



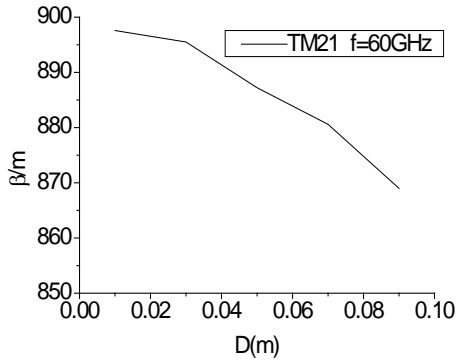


Fig. 7. The variations of the propagation constant β with respect to standard deviation of height D .

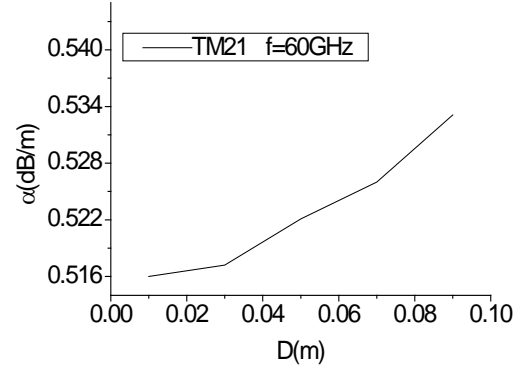
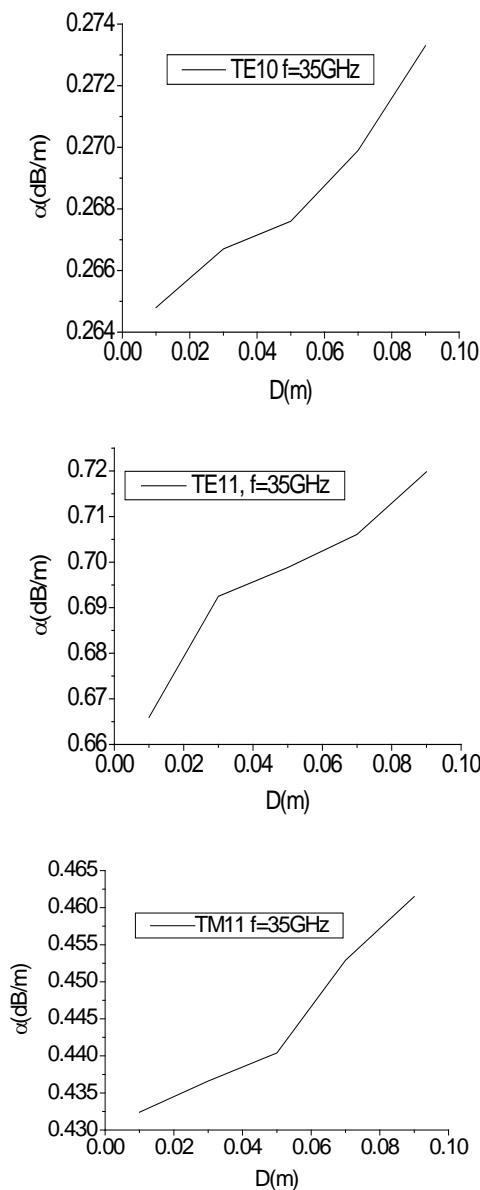


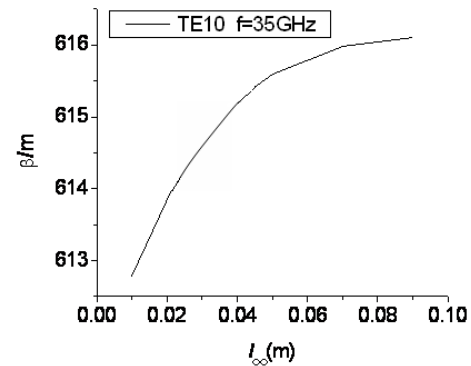
Fig. 8. The variations of attenuation constant α with respect to standard deviation of height D .



D. Effect of work frequency f

To discuss the effect of the work frequency f on the propagation constant β and attenuation constant α , we suppose conductivity of the waveguide $\sigma = 5.8 \times 10^7$ S/m, standard deviation of height $D=0.03$, and correlation length $l_{co}=0.05$. The variations of propagation constant β and attenuation constant α with respect to frequency f are shown in Figs. 11 and 12. Obviously, as the increase of f , the propagation constants β are increased and the attenuation constants α are decreased.

The dotted lines in Fig. 12 represent the variations of attenuation constant α with respect to work frequency in a smooth waveguide for every mode. It can be seen from this figure that, the variations of attenuation constant with respect to work frequency f for the rough waveguide is the same as that for the smooth waveguide.



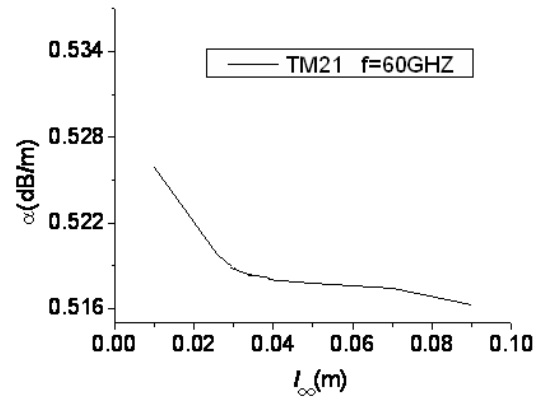
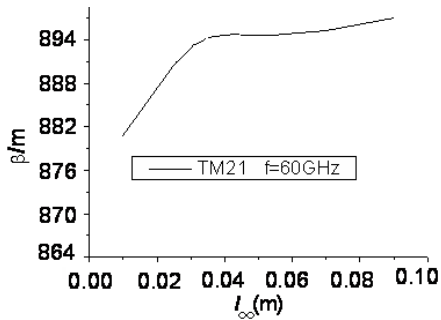
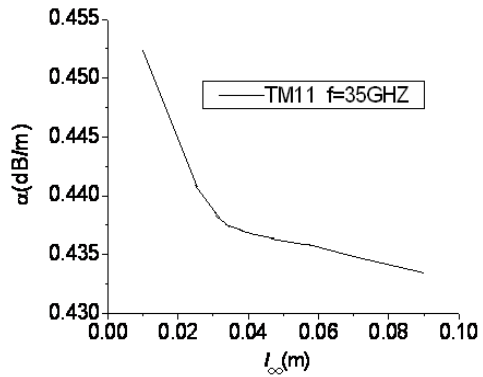
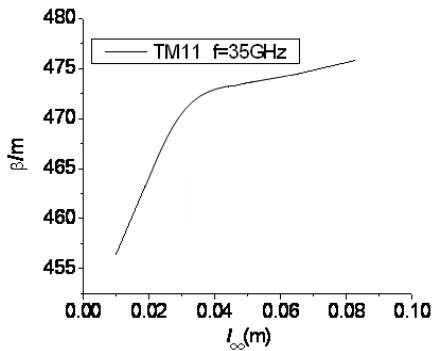
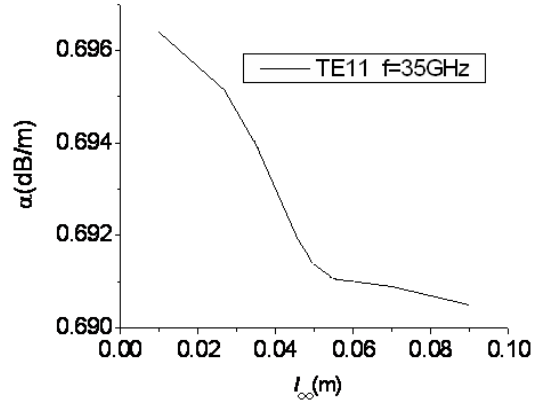
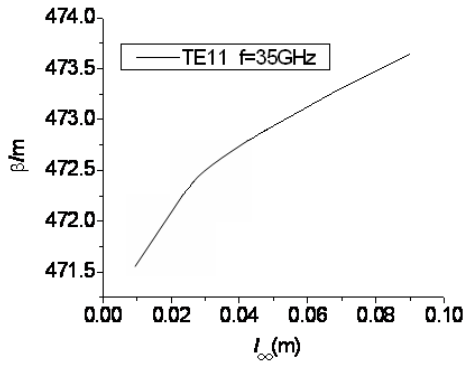
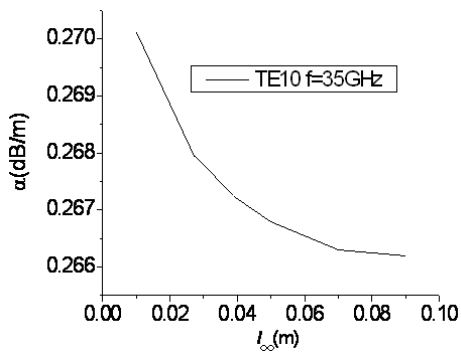


Fig. 9. The variations of the propagation constant β with respect to correlation length l_{co} .

Fig. 10. The variations of attenuation constant α with respect to correlation length l_{co} .



The discrepancy of the propagation constant β between perfect conductor waveguide and copper waveguide is defined as,

$$\beta_{er} = \frac{|\beta^p - \beta^c|}{\beta^p}, \quad (18)$$

where β^p , β^c is the propagation constant of perfect conductor waveguide and copper waveguide calculated by using integral equation method, respectively.

Similarly, the discrepancy of the attenuation constant α is defined as,

$$\alpha_{er} = \frac{|\alpha^p - \alpha^c|}{\alpha^p}, \quad (19)$$

For TE10, TE11, TM11, and TM21 modes, the β_{er} and α_{er} for different work frequency f are shown in Tables 1-4. It can be seen from these tables that, for all the modes, the discrepancies of β and α between perfect conductor waveguide and copper waveguide are decreased as the increase of the frequency f , which means that the effect of the loss metal on the propagation performance of the waveguide is decreased as the increase of frequency f .

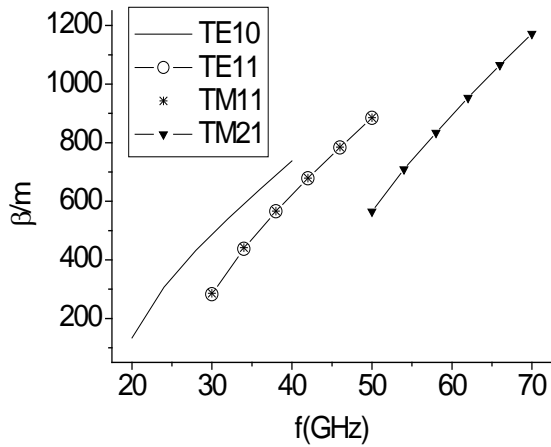


Fig. 11. The variations of the propagation constant β with respect to work frequency f

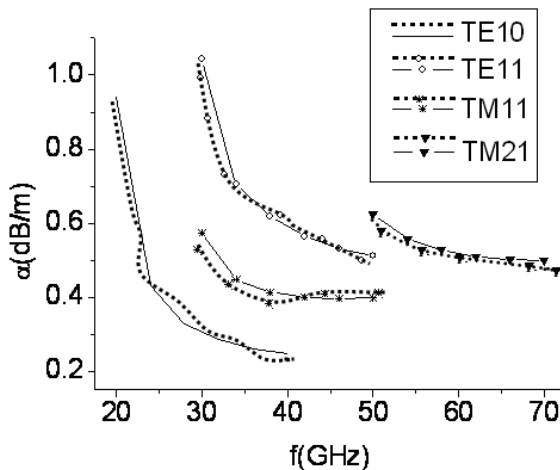


Fig. 12. The variations of attenuation constant α with respect to work frequency f

Table 1: The β_{er} and α_{er} of TE10 mode for different work frequency

f (GHz)	β_{er} (%)	α_{er} (%)
20	3.18	3.79
24	0.99	2.27
28	0.23	1.65
32	0.18	0.88
36	0.16	0.71
40	0.14	0.69

Table 2: The β_{er} and α_{er} of TE11 mode for different work frequency

f (GHz)	β_{er} (%)	α_{er} (%)
30	1.12	2.19
34	0.73	1.81
38	0.24	0.59
42	0.16	0.55
46	0.16	0.40
50	0.15	0.33

Table 3: The β_{er} and α_{er} of TM11 mode for different work frequency

f (GHz)	β_{er} (%)	α_{er} (%)
30	2.30	2.41
34	0.76	0.79
38	0.65	0.68
42	0.42	0.43
46	0.33	0.35
50	0.28	0.28

Table 4: The β_{er} and α_{er} of TM21 mode for different work frequency

f (GHz)	β_{er} (%)	α_{er} (%)
50	0.71	0.74
54	0.57	0.58
58	0.53	0.54
62	0.30	0.31
66	0.21	0.21
70	0.21	0.21

V. CONCLUSION

An integral equation method has been performed to evaluate the propagation characteristic of the random rough lossy waveguide. It has been shown that the propagation characteristic strongly depends on the frequency, the standard deviation of height and correlation length. As the correlation length and frequency increases, the propagation constant is increased and the attenuation constant is decreased; while as the increase of the standard deviation, the trends of the propagation constant and the attenuation constant are just opposite. Those results may have interesting applications for optical telecommunication and hollow dielectric film coated waveguide for THz radiation.

ACKNOWLEDGMENT

This work was supported by National Natural Science Foundations of China (No. 61001039), and also supported by the Research Fund for the Doctoral Program of Higher Education of China (20090201120030).

REFERENCES

- [1] C. D. Chen, C. K. C. Tzuang, and S. T. Peng, "Full-Wave Analysis of a Lossy Rectangular Waveguide Containing Rough Inner Surfaces," *IEEE Microwave Guided Wave Lett.*, vol. 2, pp. 0-181, 1999.
- [2] S. K. Popalghat, A. Chaudhari, and P. B. Patil, "Effect of Surface Roughness on Electromagnetic Propagation through Waveguides," *Indian Journal of pure & Applied Physics*, vol. 37, pp. 48-852, 1999.
- [3] A. M. Sua´rez, R. E. Luna, J. C. Mandujano, and J. E. Luna, "Numerical Technique to Calculate Modes in Waveguides of Arbitrarily Cross-Sectional Shape," *J. Opt. Soc. Am. A*, vol. 18, pp. 961-965, 2001.
- [4] G. A. Rubioa, A. M. Sua´rez, R.E. Lunaa, and E. T. Herna´ndezb, "Application of a New Numerical Method to Calculate TE Modes in Hollow-Conducting Waveguides," *Optical Communications*, vol. 221, pp. 301-306, 2003.
- [5] A. M. Sua´rez, U. R. Corona, and R. E. Luna, "Effects of Wall Random Roughness on TE and TM Modes in a Hollow Conducting Waveguide," *Optical Communications*, vol. 238, pp. 291-299, 2004.
- [6] Y. J. Zhao, K. L. Wu, and K. K. M. Cheng, "A Compact 2-D Full-Wave Finite-Difference Frequency-Domain Method for General Guided Wave Structures," *IEEE Trans. Microwave Theory Tech.*, vol. 50, pp. 1844-1848, 2002.
- [7] J. Li, L. X. Guo, and H. Zeng, "FDTD Investigation on Electromagnetic Scattering from Two-Dimensional Layered Rough Surfaces," *Applied Computational Electromagnetics Society (ACES) Journal*, vol. 25, pp. 450-457, May 2010.
- [8] L. D. Rienzo, N. Ida, and S. Yuferev, "Surface Impedance Boundary Conditions of High Order of Approximation for the Finite Integration Technique," *Applied Computational Electromagnetics Society (ACES) Journal*, vol. 22, pp. 53-59, Mar. 2007.
- [9] B. Z. Wang, X. HW, and W. Shao, "2D Full-Wave Finite-Difference Frequency-Domain Method for Lossy Metal Waveguide," *Microw. Opt. Tech.. lett.*, vol. 42, pp. 158-161, 2004.
- [10] W. H. Press, S. A. Teukolsky, W. T. Vetterling, and B. P. Flannery, *Numerical Recipes in FORTRAN*, Cambridge University Press, Cambridge, UK, 1992.